Characterization of the Ligand and DNA Binding Properties of a Putative Archaeal Regulator ST1710[†]

Linliang Yu, Jun Fang, and Yinan Wei*

Department of Chemistry, University of Kentucky, Lexington, Kentucky 40506-0055

Received September 1, 2008; Revised Manuscript Received January 19, 2009

ABSTRACT: While a rich collection of bacterium-like regulating proteins has been identified in the archaeal genome, few of them have been studied at the molecular level. In this study, we characterized the ligand and DNA binding properties of a putative regulator ST1710 from the archaeon *Sulfolobus tokodaii*. ST1710 is homologous to the multiple-antibiotic resistance repressor (MarR) family bacterial regulators. The protein consists of a ligand binding site, partially overlapping with a winged helix−turn−helix DNA binding site. We characterized the interactions between ST1710 and three ligands, salicylate, carbonyl cyanide *m*-chlorophenylhydrazone (CCCP), and ethidium, which bind to bacterial MarRs. The binding affinities of the ligands for ST1710 were comparable to their affinities for the bacterial MarRs. The ligand binding was temperature sensitive and caused conformational changes in ST1710. To investigate the effect of ligand binding on the interaction between ST1710 and DNA, we fluorescently labeled a 47mer dsDNA (ST1) containing a putative ST1710 recognition site and determined the dissociation constant between ST1 and ST1710 using the fluorescence polarization method. The binding affinity almost doubled from 10 °C (K_d = 618 ± 34 nM) to 30 °C (K_d = 334 ± 15 nM), and again from 30 to 50 °C (K_d = 189 ± 9 nM). This result suggests that under the natural living condition (80 °C) of *S. tokodaii*, the binding affinity might increase even further. The presence of CCCP and salicylate suppressed ST1710−ST1 interaction, indicating that ST1710 functioned as a repressor.

Among the three kingdoms of life, archaea, bacteria, and eukaryotes, gene transcription and regulation in the archaea are the least understood. The gene transcription and translation processes in archaea share characteristics with those of both eukaryotes and bacteria. The basal component of archaeal transcriptional machinery is similar to that of eukaryotes (*1*−*4*). For example, the archaeal RNA polymerase has a multisubunit structure that resembles the eukaryotic polymerase II (*5*); the promoter region of the archaea contains a T/A rich region that resembles the TATA box of the eukaryotes, and the archaea also have eukaryote-like transcription factors that bind and promote transcription (*1, 6*−*8*).

While a comprehensive picture of the archaeal basal transcription mechanism is emerging, understanding of the regulatory system is still sketchy. With an increasing number of archaeal genomes being sequenced, it is becoming clear that the archaea have an abundance of putative DNA binding proteins resembling bacterial-type regulators (*7, 9*−*11*). However, only a handful of these regulators have been investigated and even fewer characterized at the molecular level. MarR family transcriptional regulators were first identified by George and Levy in multidrug resistant strains of *Escherichia coli* in 1983 (*12, 13*). Now homologues of MarR can be found throughout the domains of bacteria and archaea (*14, 15*). The MarR-type transcriptional regulators in bacteria play critical roles in the regulation of cellular functions involving the aromatic catabolic pathways and the response to virulence factors and environmental stresses (for a recent review, see ref *16*). MarR regulators bind to their cognate dsDNA sequences as homodimers. The interaction between MarR and DNA is modulated by specific lipophilic compounds, including salicylate, ethidium, and CCCP[1] (Figure 1A). Crystal structures of several MarR regulators have been obtained, either as apoproteins [MexR from *Pseudomonas aeruginosa* (*17*), SlyA from *Enterococcus faecalis* (*18*), and MTH313 from *Methanobacterium thermoautotrophicum* (*19*)], in complex with the cognate dsDNA oligonucleotide fragment [OhrR from *Bacillus subtilis* (*20*)], or in complex with salicylate [MarR from *E. coli* (*21*) and MTH313 from *M. thermoautotrophicum* (*19*)]. However, the DNA-complexed and ligand-complexed structures are not yet available simultaneously for the same protein to facilitate direct comparison. An allosteric regulation mechanism has been proposed on the basis of the observation that the four dimers in the crystallographic asymmetric unit of MexR had different conformations, in which an open state (presumably DNA binding) and a closed state (presumably drug binding)

[†] This research was supported by a University of Kentucky faculty start-up grant.

* To whom correspondence should be addressed: 305 Chemistry-Physics Building, University of Kentucky, Lexington, KY 40506-0055. Telephone: (859) 257-7085. Fax: (859) 323-1069. E-mail: yinan.wei@uky.edu.

[1] Abbreviations: CCCP, carbonyl cyanide *m*-chlorophenylhydrazone; CD, circular dichroism; ESI-MS, electrospray ionization mass spectrometric; FITC, fluorescein isothiocyanate; IPTG, isopropyl β-D-thiogalactopyranoside; LC, liquid chromatography; MarR, multiple antibiotic resistance repressor; PCR, polymerase chain reaction; TNM, tetranitromethane.

10.1021/bi801662s CCC: $40.75
Published on Web 01/23/2009

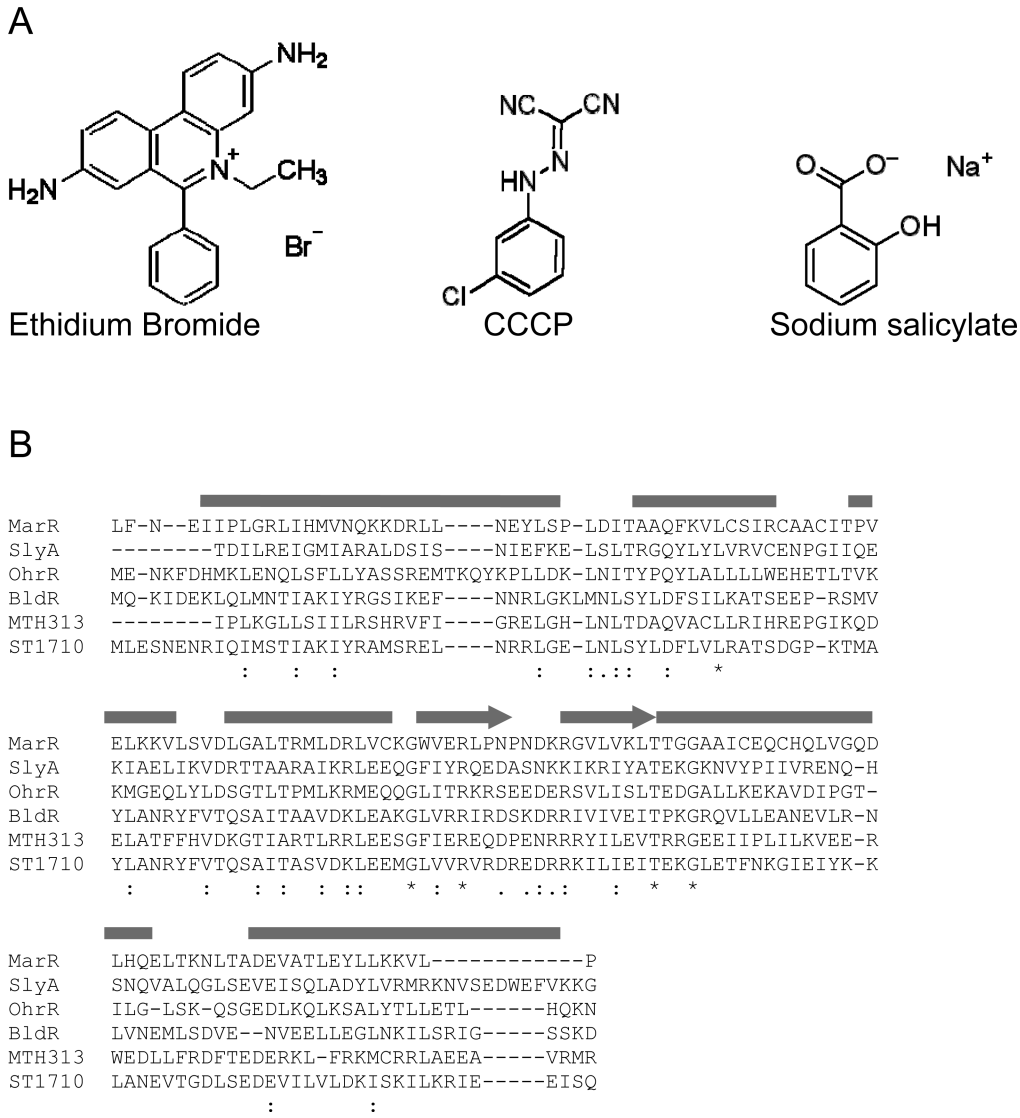

FIGURE 1: (A) Chemical structures of the ligands used in this study. (B) Sequence alignment of ST1710 with representative MarR family proteins from bacteria (MarR, SlyA, and OhrR) and archaea [MTH313 and BldR (*41*)]. The alignment was performed using the online server of Tcoffee (*45*). The conserved, highly conserved, and identical residues are denoted with periods, colons, and asterisks, respectively. The secondary structure elements are indicated as bars (α-helix) and arrows (*β*-strand).

could be identified (*17*). Recently, crystal structures of MTH313 were determined both in the apo state and in complex with salicylate (*19*). A comparison of these two structures illustrated a large conformational change in the DNA binding lobe, further supporting the notion that protein conformational changes are involved in the mechanism of regulation.

ST1710 from *Sulfolobus tokodaii* is a putative MarR-like regulator. The crystallographic structure of ST1710 has been determined in its apo form (*22, 23*). The structures of MarR family proteins are very similar, although very little conserved residues present in their sequences (Figure 1B). On the basis of the structural similarity with the bacterial MarR proteins, ST1710 is expected to function similarly as well. While the majority of the MarR regulators studied are repressors, there are also activators. The repressors bind to their target DNA site to block the transcription of the cognate genes in the absence of the effector. When its cytoplasmic concentration reaches a critical level, the effector binds to the ligand binding site of the repressor and disrupts the interaction between the protein and DNA, and subsequently initiates the transcription of the genes. In contrast, for activators the effector binding promotes favorable interaction with the target DNA to initiate transcription.

The effector binding has been characterized for a couple of bacterial MarR family regulators. These effectors are usually lipophilic compounds with planar structures, such as ethidium, salicylate, and CCCP (Figure 1A). However, no detailed biophysical characterization of the ligand binding to archaeal MarR-like regulators has been reported. In this study, we characterize the binding of the above-mentioned ligands to ST1710. We examine the binding affinity, stoichiometry, and resultant protein conformational change. We also investigate the effect of ligand binding on the interaction between ST1710 and a double-stranded DNA oligonucleotide containing the putative ST1710 binding site (*22*). Our study indicates that the recombinant ST1710 bound to all three ligands, and this binding disrupted the interaction between the protein and DNA.

MATERIALS AND METHODS

Cloning, Mutation, Expression, and Purification. The *ST1710* gene was amplified by polymerase chain reaction (PCR) from plasmid STLGR15159 (National Institute of Technology and Evaluation, Tokyo, Japan). The following primer pairs were used for PCR: forward, 5′-CACCATGTTAGAAAGTAATGAAAACAGAATAC-3′; and reverse, 5′-TCACTGACTAATTTCCTCAATTCTTTTC-3′. The PCR product was inserted into the TOPO TA expression vector following the manufacturer's instruction (Invitrogen, Carlsbad, CA) to generate plasmid pTOPO-ST1710, which introduced a polyhistidine tag at the N-terminus of the protein. Plasmid pTOPO-ST1710 was used to transform *E. coli* strain Rosetta2 (EMD Biosciences, San Diego, CA) for protein production. The cells were grown at 37 °C in Luria-Bertani (LB) medium containing 100 μg/mL ampicillin and 34 μg/mL chloramphenicol to an OD_{600} of 0.6 and then induced with 1 mM isopropyl β-D-thiogalactopyranoside (IPTG). Three hours after the induction, the cells were harvested by centrifugation at 6000*g* for 10 min. The cell pellet was resuspended in buffer A [50 mM HEPES buffer and 200 mM NaCl (pH 7.5)] and lysed by sonication on ice for 5 min with 10 s on−off intervals. The cell debris was separated from the supernatant by centrifugation at 10000*g* for 15 min. The same centrifugation condition was used throughout the purification steps unless otherwise indicated. The cleared lysate was incubated at 70 °C for 45 min, followed by centrifugation to remove the heat-denatured impurities. The supernatant was incubated with the Ni-NTA resin (Qiagen, Huntsville, AL) with shaking at room temperature for 1 h, then washed with buffer B [50 mM HEPES buffer, 200 mM NaCl, and 35 mM imidazole (pH 7.5)], and finally eluted with buffer C [50 mM HEPES buffer, 200 mM NaCl, and 500 mM imidazole (pH 7.5)]. Purified ST1710 was dialyzed extensively against buffer A to remove the excess imidazole. ST1710 mutants containing a single tyrosine (Tyr) to tryptophan (Trp) mutation were constructed using the QuikChange site-directed mutagenesis kit (Stratagene, La Jolla, CA). The primers used to construct Y55W were 5′-GACGGTCCAAAAACAATGGCATGGTTAGCAAATAGATATTTCGTT-3′ and its complementary sequence. The primers used to construct Y60W were 5′-GCATATTTAGCAAATAGATGGTTCGTTACACAATCAGCAATA-3′ and its complementary sequence. Expression and purification procedures for the mutants were the same as those of the wild-type protein.

The purity of the protein was analyzed using sodium dodecyl sulfate−polyacrylamide gel electrophoresis. Protein samples were separated on a 20% homogeneous polyacrylamide Phast gel (Phast System, GE Healthcare, Waukesha, WI) and visualized with Coomassie Blue stain. Molecular weight standards (Benchmark Protein Markers) were obtained from Invitrogen. Protein concentrations were determined by UV absorbance at 280 nm using extinction coefficients of 8940 and 12950 M^{-1} cm^{-1} for the wild-type and mutant proteins, respectively.

Circular Dichroism (CD) Spectroscopy. The CD experiment was performed on a JASCO J-810 spectrometer (JASCO) with a 0.1 cm path length cuvette. ST1710 was dialyzed overnight into a Tris buffer (20 mM, pH 8.0) for the CD measurement. Blank scans were performed using the exterior dialysis buffer and subtracted from the measured data.

Fluorescence Spectroscopy. Fluorescence polarization experiments and wavelength scans were performed using a Perkin-Elmer LS-55 fluorescence spectrometer (Perkin-Elmer, Waltham, MA). For the Trp fluorescence measurement, the protein was dialyzed overnight into a Tris buffer (20 mM, pH 8.0). The excitation wavelength was 280 nm. The protein and ethidium concentrations were 1 and 5 μM, respectively. For the fluorescence polarization studies of fluorescein isothiocyanate (FITC)-labeled ST1, the excitation and emission wavelengths were 492 and 515 nm, respectively. The forward oligonucleotide of ST1 (5′-AATGAAAACAGAATACAAATAATGTCAACAATAGCAAAAATATACAG-3′) was labeled with FITC at the 5′-terminus (all DNA oligonucleotides, including FITC-labeled ones, were obtained from Operon, Huntsville, AL). The forward and reverse oligonucleotides were mixed at a 1:1 ratio at a final concentration of 100 μM in a 500 μL reaction buffer [10 mM HEPES (pH 7.5) and 50 mM NaCl]. The sample was protected from light and incubated in a boiling water bath for 10 min, and then the water bath (2 L) together with the sample was cooled slowly to room temperature. The annealed double-stranded DNA was used throughout the binding experiment. The reaction buffer was supplemented with 1 μg/mL calf thymus DNA to eliminate the nonspecific binding (*24*). To assess the binding of ethidium to ST1710, the excitation and emission wavelengths for the fluorescence polarization experiment were 520 and 600 nm, respectively. The same excitation wavelength was used to collect the ethidium emission spectra.

Tetranitromethane (TNM) Nitration. The TNM nitration procedure was performed following the published method (*25*). Briefly, TNM was added to a reaction buffer [0.5 M Tris-HCl (pH 8.0)] containing 62.5 μM ST1710 at a final concentration of 750 μM. Ethidium bromide was added when indicated to the reaction mixture at a final concentration of 100 μM before the addition of TNM. The reaction mixture was incubated at 35 °C for 1 h and then passed through desalting columns twice to remove the excess TNM and ethidium. The nitrated Tyr was quantified using the absorbance at 428 nm with an extinction coefficient of 4200 cm^{-1} M^{-1} (*26*). The concentration of the protein was determined using the Bradford assay. The number of nitrated Tyr residues per protein molecule was estimated by the ratio of these two concentrations.

Data Fitting. Two fitting models were used to derive the binding dissociation constants from the titration data. Origin 5.0 (OriginLab, Northampton, MA) was used for data fitting. All signals were corrected for dilution.

The Hill equation was used to fit the data when the concentration of the ligand (ST1 or ethidium), which was kept constant during the titration, was much smaller than the concentration of ST1710. Under such circumstances, the concentration of the protein−ligand complex was very small compared to the total protein concentration. Thus, the total protein concentration could be used to replace the free protein concentration ([S]) during the fitting without causing significant error:

$$\Delta P = \Delta P_{max} \times \frac{S^n}{K_d^{\,n} + S^n}$$

ΔP is the polarization increment upon the addition of ST1710, ΔP_{max} is the maximum polarization increment when the protein concentration ([S]) approaches infinity, and n is the Hill coefficient, with $n > 1$ describing a positive cooperativity and $n < 1$ describing a negative cooperativity. K_d is the dissociation constant.

A noncooperative 1:1 binding model was used when the concentration of the complex cannot be ignored (*24*), such as in the case of binding between ST1710 and CCCP:

$$P + L \rightarrow PL$$

$$K_d = \frac{[P_f][L_f]}{[PL]}$$

$$[P_f] = [P_T] - [PL],\ [L_f] = [L_T] - [PL]$$

$$K_d = \frac{([P_T] - [PL])([L_T] - [PL])}{[PL]}$$

$[P_T]$, $[P_f]$, $[L_T]$, $[L_f]$, and $[PL]$ are concentrations of the total protein, free protein, total ligand, free ligand, and protein−ligand complex, respectively. Solving for $[PL]$:

$$[PL]^2 - ([P_T] + [L_T] + K_d)[PL] + [P_T][L_T] = 0$$

$$[PL] = \frac{[P_T] + [L_T] + K_d - \sqrt{([P_T] + [L_T] + K_d)^2 - 4[P_T][L_T]}}{2}$$

For CCCP binding, the ellipticity at 325 nm (y) is proportional to the concentration of the protein−CCCP complex ([PL]). The change in y as a function of the total ligand concentration x ($x = [L_T]$) can be represented as

$$\frac{y - Y_{min}}{Y_{max} - Y_{min}} = \frac{[PL]}{[P_T]} = \frac{[P_T] + x + K_d - \sqrt{([P_T] + x + K_d)^2 - 4[P_T]x}}{2[P_T]}$$

$$y = \frac{(Y_{max} - Y_{min})[([P_T] + x + K_d) - \sqrt{([P_T] + x + K_d)^2 - 4[P_T]x}}{2[P_T]} + Y_{min}$$

During the experiment, small aliquots of CCCP were titrated into a solution of ST1710. The dilution effect was kept to be less than 2%, so $[P_T]$ can be treated as a constant without causing significant error in fitting. Y_{min} and Y_{max} correspond to the theoretical ellipticities at CCCP concentrations of zero and infinity, respectively. The y versus x data were fitted with three floating parameters, K_d, Y_{min}, and Y_{max}.

RESULTS AND DISCUSSION

Ligand Binding to ST1710. All MarR-type regulators characterized thus far bind to effectors. Several small molecules have been shown to bind to the MarR family regulators. We chose three representative ligands to study effector binding to ST1710, including a cationic molecule (ethidium), an anionic molecule (salicylate), and a neutral molecule (CCCP) (Figure 1A).

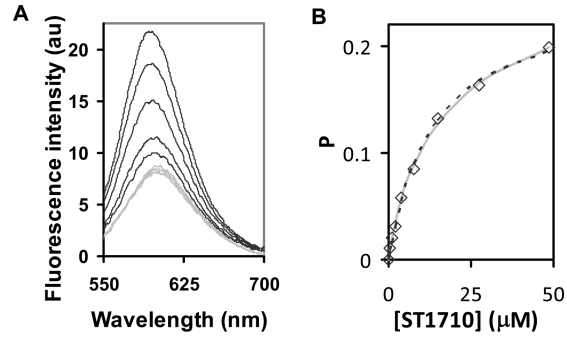

FIGURE 2: Binding of ethidium with ST1710. (A) The intrinsic fluorescence of ethidium was used to moniter its binding to ST1710 at different temperatures. Two traces were collected at each temperature, one for ethidium alone (1 μM) (gray) and the other for ethidium (1 μM) with protein (20 μM) (black). From top to bottom, the black traces were collected at 10, 20, 30, 40, and 50 °C, respectively. The effect of temperature on the fluorescent emission of free ethidium was very small, so the gray traces of the five temperatures superimposed onto each other in the bottom part of the figure. The increase in temperature drastically decreased the binding affinity of ethidium for ST1710. (B) At 10 °C, the fluorescence polarization changes of an ethidium solution upon addition of ST1710 were recorded and fitted with both the Hill equation (solid gray line) and the noncooperative 1:1 binding modle (dotted black line). Fitting parameters are summarized in Table 1.

The binding of ethidium to ST1710 was assessed directly using the intrinsic fluorescence of ethidium. When ethidium was bound with protein, its fluorescence emission peak blue-shifted and increased in intensity (Figure 2A, black traces). Since *S. tokodaii* is a thermophile living at 80 °C, we examined the effect of temperature on ethidium−ST1710 binding with 10 °C intervals from 10 to 50 °C (Figure 2A). The interaction between ethidium and ST1710 became weaker at higher temperatures. To determine the binding affinity between ethidium and ST1710, we titrated the protein into a solution of ethidium as described in Materials and Methods. At 10 °C, fitting the binding data with the Hill equation yielded a dissociation constant of 19.1 ± 4.6 μM (Figure 2B, solid gray line). The n value was found to be 0.88 ± 0.07, indicating a lack of binding cooperativity. For the purpose of comparison, an alternative noncooperative 1:1 binding model was also used to fit the data (Figure 2B, dotted black line). The dissociation constant derived from this fitting model was 13.7 ± 1.2 μM. The two curves superimposed well, and the two K_d values were within reasonable agreement with each other, indicating the validity of the fitting.

To evaluate the potential contribution of the protein structural change to the observed effect of temperature on binding, we collected the CD spectra of ST1710 at 10 and 50 °C. The structural stability of a helical protein is usually monitored by the disappearance of the helical structure in the far-UV region. We collected the far-UV CD spectra at 190−260 nm (Figure 3). The protein was highly α-helical, as expected from the crystal structure. The two spectra exhibited very few differences, indicating the protein was stable at 50 °C. Such observation was not surprising as the protein can tolerate being heated at 80 °C for at least 30 min or 90 °C for 10 min (*22, 23*).

Next, CD spectroscopy was used to evaluate the ST1710 structural change associated with ligand binding. The potential change in protein secondary structure upon ligand binding cannot be monitored in the far-UV region (<260 nm),

Table 1: Fitting Parameters for ST1710−Ligand and ST1710−DNA Binding

Ligand Binding				
ligand	protein	K_d (apparent)	n^a	ref
salicylate	MarR	2 mM		*42*
	ST1710	∼1 mM[b]		this work
ethidium	ST1710	19.1 ± 4.6 μM (Hill equation)	0.88 ± 0.07	this work
		13.7 ± 1.2 μM (noncooperative binding model)	/	
CCCP	EmrR	5−25 μM		*43*
	EmrR	2 μM		*44*
	ST1710	57.0 ± 7.0 μM	∼1	this work

DNA Binding		
temp (°C)	n^a	K_d (nM)
10	1.12±0.05	618 ± 34
30	1.13±0.05	334 ± 15
50	1.06±0.04	189 ± 9

[a] *n* is calculated per protein monomer. [b] Estimated from its inhibitory effect in Figure 8B.

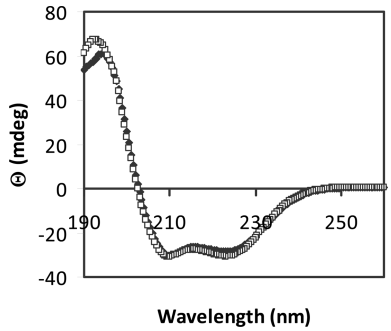

FIGURE 3: Circular dichroism study of ST1710. The secondary structure of ST1710 is highly α-helical, consistent with its crystal structure. The conformation of the protein changed little when the temperature increased from 10 °C (□) to 50 °C (◆).

due to the strong absorption by the ligands. Instead, the near-UV CD spectra (260−350 nm), which reveal information about a protein's tertiary structure, were collected for the free protein, free ligands, and the protein−ligand complexes (Figures 4 and 6). Aromatic residues, especially Trp, are major contributors to the near-UV CD signal. Since ST1710 has no intrinsic Trp, a high protein concentration had to be used (300 μM) to achieve an adequate signal-to-noise ratio for the spectrum. The ligand concentration should be sufficiently high to form a significant amount of protein complex to facilitate detection, while at the same time not so high that the ligand absorption would deteriorate the CD signal. In the case of ethidium, its absorption at 300 μM (to achieve a 1:1 molar ratio to the protein) led to a poor signal-to-noise ratio, so the spectra shown in Figure 4A were acquired with 150 μM ethidium. At a ligand-to-protein ratio of 0.5:1, only a portion of the protein will bind to ethidium. However, there was still a clear difference between the CD traces of the apoprotein (□) and the protein−ethidium mixture (◆) in the wavelength region between 260 and 275 nm, supporting the notion that ethidium binding induced protein conformational change.

Salicylate absorbed much less in the wavelength range studied and could be used at 2 mM to achieve a ligand-to-protein ratio of 20:3 (Figure 4B). The differences between the protein (□) and protein−salicylate mixture (◆) traces

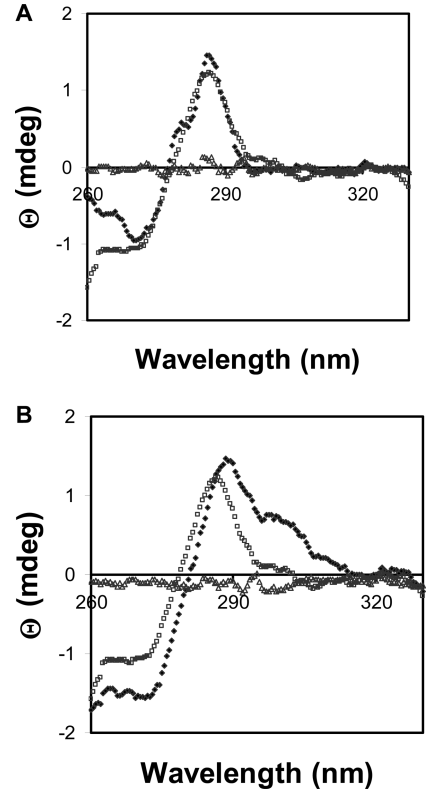

FIGURE 4: ST1710 conformational change induced by the binding of ethidium (A) and salicylate (B) at 50 °C. CD spectra of ST1710 (□), ligand (△), and ST1710 bound with ligand (◆). Concentrations of the protein, ethidium, and salycilate used in the experiments were 300, 150, and 2000 μM, respectively.

were apparent. The major positive peak shifted from 275 to 280 nm, and the minor positive peak at 300 nm became more predominant. Clearly, the binding of salicylate led to a protein conformational change.

Due to the limitations of experimental conditions as discussed above, the near-UV CD spectra exhibited only minor changes after the addition of ethidium (Figure 4A). To further evaluate the effect of ethidium binding, we monitored its influence on the Trp fluorescence. The Trp fluorescence is very sensitive to the environment and thus has been used broadly as a reporter for protein conformational change. Ethidium has no significant fluorescence emission under the experimental condition used for this study. We first performed site-directed mutagenesis experiments to introduce a single Trp into the protein sequence, as ST1710 has no intrinsic Trp. Ideally, the reporter Trp should be placed at a location that experiences the most dramatic structural change following ligand binding. In an effort to identify the proper position for the mutation, we superimposed the structures of apo ST1710 with apo and salicylate-bound MTH313 (Figure 5A). As expected, the overall structure of ST1710 was very similar to that of MTH313. In the structure of ST1710, two tyrosines (Y55 and Y60) were found to be close to the corresponding ligand binding site in MTH313. Therefore, these two tyrosines were chosen to be replaced with Trp. We constructed two single Tyr to Trp mutants (Y55W and Y60W) and monitored their Trp fluorescence changes following ethidium binding (Figure 5B,C). The fluorescence of wild-type ST1710 was also acquired under the same experimental condition as a reference (Figure 5B). The fluorescence intensity of wild-type

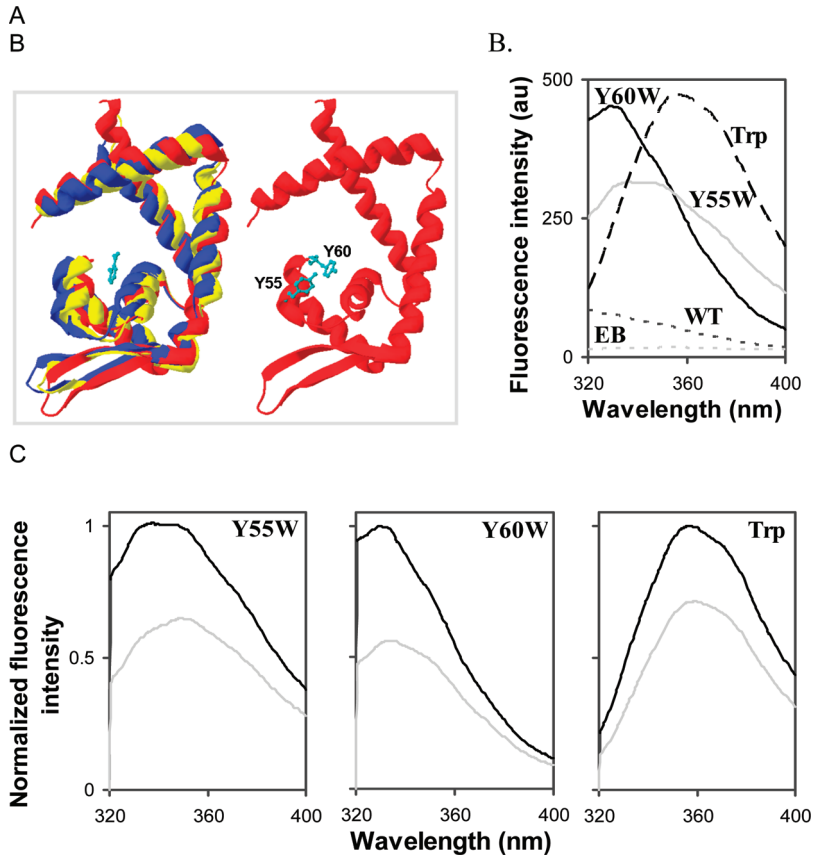

FIGURE 5: Effect of ethidium binding on the Trp fluorescence emission. (A) The left panel shows the superimposition of the crystal structures of apo MTH313 (blue), MT313 in complex with salicylate (yellow, with salicylate shown as a cyan ball-and-stick model), and ST1710 (red). Protein Data Bank entries 3BPV (apo MTH313), 3BPX (MTH313−salicylate complex), and 2EB7 (ST1710) were used to create this figure. The right panel shows the structure of ST1710, with residues Y55 and Y60 shown as cyan ball-and-stick models. (B) Fluorescence emission spectra of mutants Y60W (solid black line), Y55W (solid gray line), wild-type ST1710 (dotted black line), Trp (dashed black line), and ethidium bromide (dotted gray line). The excitation wavelength was 280 nm. The concentrations of the proteins, Trp, and ethidium were 1, 1, and 5 μM, respectively. (C) Normalized fluorescence emission spectra of mutants Y55W and Y60W and Trp in the absence (black) and presence (gray) of ethidium bromide. The experimental condition was the same as described above. The spectra in each panel were normalized to the maximum emission intensity of the sample in the absence of ethidium.

ST1710 was very small in the wavelength region examined, as expected for a protein without intrinsic Trp. As a control experiment, we examined the effect of the presence of ethidium on the fluorescence emission of the free amino acid Trp under the same experimental condition (Figure 5C). Ethidium quenched the fluorescence of both the ST1710 mutants and the free amino acid Trp. However, in the latter case, the quenching involved an intensity drop of only approximately 30%, with very little wavelength shift of the emission peak. For mutants Y55W and Y60W, the intensities dropped by approximately 35 and 40%, respectively, and the emission maxima also red-shifted. In addition, the changes caused by ethidium binding on the fluorescence spectra of Y55W and Y60W were different, supporting the notion that protein conformational changes were associated with ethidium binding. However, the potential contributions from the direct Trp−ethidium interactions could not be completely excluded. The bound ethidium might be in the proximity of W55 and W60, and thus, the binding of ethidium might have changed the chemical environment of the reporter Trp and therefore produced the observed changes in fluorescence emission.

We performed additional experiments to further confirm that protein conformational change occurred. TNM specifically nitrates Tyr to form 3′-nitrotyrosine (*26, 27*). The susceptibility of a specific Tyr in a protein sequence to the TNM nitration has been exploited to assess the solvent accessibility of the corresponding residue (*25, 27*). Wild-type ST1710 was treated with TNM in the presence or absence of 100 μM ethidium bromide. The modified protein was separated from the excess TNM and ethidium bromide by passing the reaction mixture through a desalting column. Finally, the number of Tyr residues nitrated per protein was estimated as described in Materials and Methods. ST1710 has five tyrosines. A 12-fold TNM-to-protein molar excess (2.4-fold molar excess vs Tyr) was used during the experiment. In the absence of ethidium, approximately two tyrosines per protein molecule were nitrated. The presence of ethidium in the nitration step reduced the efficiency of nitration by approximately 30%, with 1.4 tyrosines modified per protein (data not shown). To identify the exact site of modification, we submitted TNM-modified ST1710 to the University of Kentucky Mass Spectrometry Facility for MS analysis. Gel pieces containing the modified protein were digested with trypsin and then subjected to LC−ESI-MS/MS analysis. Resulting MS/MS spectra were searched against archaeobacteria proteins in the NCBInr database using the Mascot search engine (Matrix Science) allowing nitrotyrosine modification. ST1710 was identified as the top hit. ST1710 contains five tyrosines: Y19, Y37, Y55, Y60, and Y111.

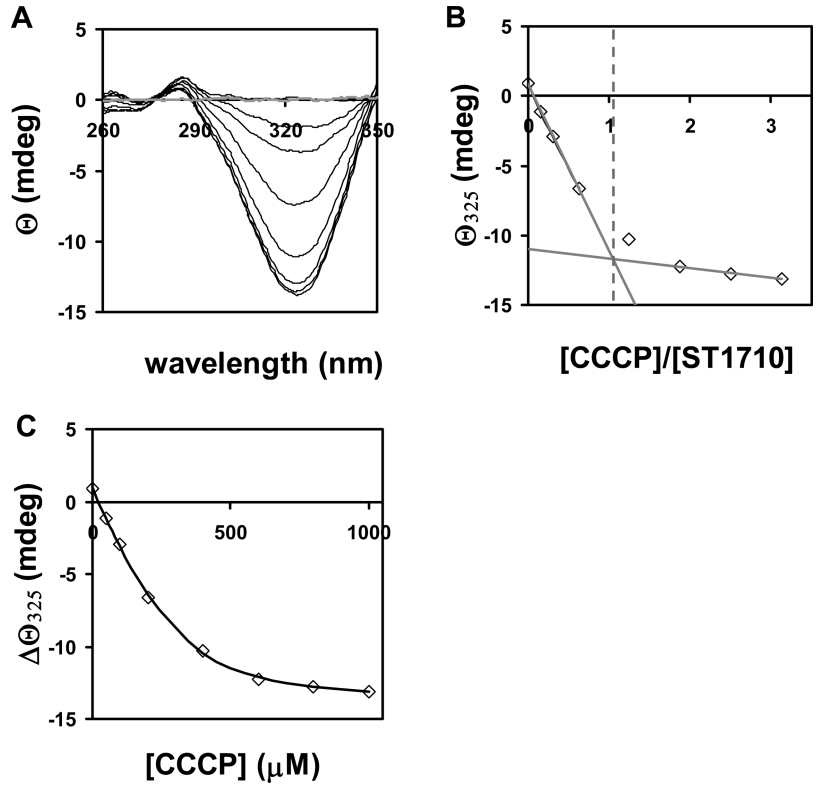

FIGURE 6: Binding study of CCCP and ST1710 with CD spectroscopy. (A) Black traces from top to bottom are for 300 μM ST1710 with 0, 50, 100, 200, 400, 600, 800, and 1000 μM CCCP, respectively. The gray trace is for 1000 μM CCCP alone. (B) The ellipiticity at 325 nm in panel A was plotted vs the molar ratio of CCCP to ST1710 to determine the stoichiometry of binding. Liner regressions of the data points from the first four (0, 50, 100, and 200 μM) and last three (600, 800, and 1000 μM) concentrations crossed at a ligand-to-protein ratio of ~1:1 (dotted gray line). (C) The ellipiticity at 325 nm was plotted vs the concentration of CCCP and fitted with the 1:1 binding model.

Peptide fragments containing four of them (Y37, Y55, Y60, and Y111) were identified in the MS/MS spectra. Y55 only presented in the nitrated form, suggesting that this Tyr was nitrated to a very high extent. Y37, Y60, and Y111 presented in both the unmodified and nitrated forms. Due to the limited quantification capability of MS, the extent of nitration could not be reliably derived for Y37, Y60, and Y111. The nitration state of Y19 was also unknown, as the peptide fragment containing Y19 could not be observed in the spectra. As a summary, at least four tyrosines (Y37, Y55, Y60, and Y111) were nitrated in ST1710, with Y55 modified to a very high extent. Nitration was not localized to two specific tyrosines, although statistically two tyrosines were modified per protein. The extent of modification was 30% lower in the presence of ethidium. Due to the limited quantification capability of the experiment, it would be difficult to attribute the 30% decrease in nitration to any specific Tyr. Most likely, it was a combined effect of all the modified tyrosines.

The CD spectra for CCCP binding are very intriguing (Figure 6). Neither 1 mM CCCP alone (gray) nor the ST1710 alone (black, first line from the top, overlaps partially with the gray line) had a significant signal at around 325 nm (Figure 6A). However, a negative peak emerged at 325 nm with the addition of CCCP to ST1710, which grew with the increase in the CCCP concentration and finally reached saturation. The near-UV CD profiles of proteins have been well characterized, and the signals are attributed to aromatic residues (Trp, Tyr, and Phe) and a disulfide bond (*28, 29*). There is no intrinsic Trp or Cys in ST1710. Tyr usually has a peak between 275 and 282 nm, and Phe shows sharp fine structures between 255 and 270 nm (*30*). On the basis of this analysis, the changes of the CD signal between 260 and 270 nm might come from the protein conformational change. However, the negative peak at 325 nm most likely came from the protein-bound CCCP, which gained a certain degree of chirality in the asymmetric binding pocket. Such observations are well-documented for certain ligands and cofactors that have little CD signal in their free forms, while producing large ellipticity readings once bound with proteins (*31*−*35*). The ellipticities at 325 nm in Figure 6A were plotted versus the molar ratio of CCCP to ST1710 (Figure 6B). A clear inflection point occurred at the CCCP-to-ST1710 molar ratio of 1:1, strongly suggesting a binding stoichiometry of one CCCP per ST1710 monomer. The 1:1 binding model was then used to fit the binding curve, yielding a dissociation constant of 57.0 ± 7.0 μM (Figure 6C).

Piecing together information obtained from the binding studies of these three ligands, we found that ST1710 bound to the ligands at affinities close to those of the bacterial MarR proteins (Table 1). ST1710 formed homodimers in solution, characteristic of MarR family members (*22*). One molecule of CCCP was found to bind with each ST1710 subunit; however, no cooperativity was observed between the two binding sites in a ST1710 dimer. Similarly, no cooperativity was observed for the binding of ethidium.

Effect of Temperature on ST1710−*DNA Interaction.* A MarR transcriptional regulator can be either a repressor or an activator. ST1710 is expected to be a repressor, based on its high degree of homology with the *E. coli* MarR repressor EmrR (*23*). Kumarevel et al. identified a putative DNA

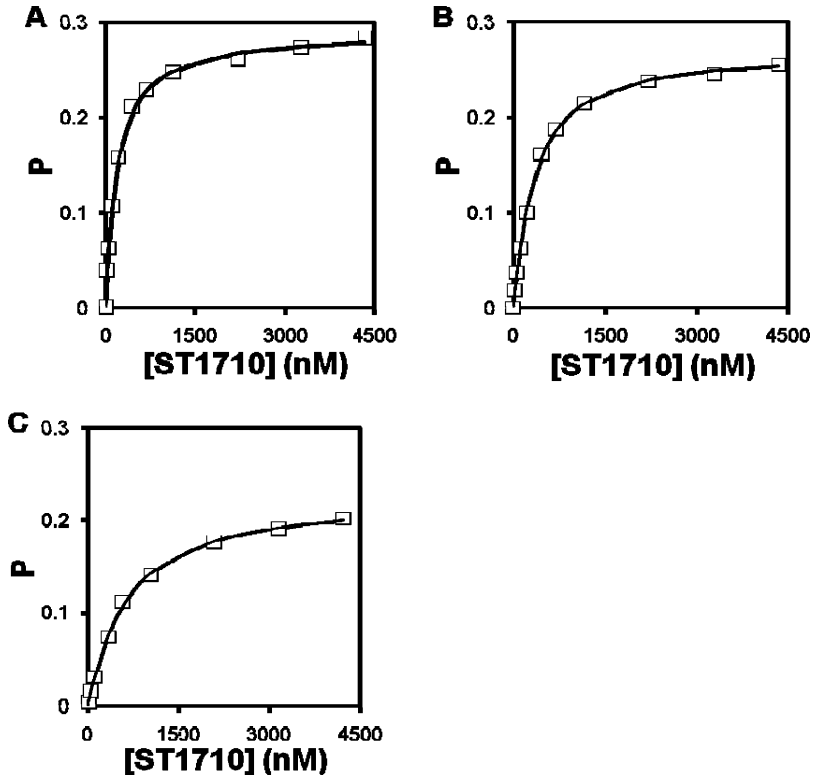

FIGURE 7: Effect of temperature on the binding between ST1710 and ST1. ST1710 was titrated into a binding buffer [10 mM HEPES, 50 mM NaCl (pH 7.5), and 1 μg/mL calf thymus DNA] containing 5 nM F-ST1 at 50 (A), 30 (B), and 10 °C (C). Fluorescence polarization was monitered with an excitation wavelength of 492 nm and an emission wavelength of 515 nm. The binding data were fitted with the Hill equation for dissociation constant K_d and Hill coefficient n (summarized in Table 1).

binding sequence (ST1) for ST1710 through scanning the local sequence of the *S. tokodaii* genome for homology with the *ohrA* promoter sequence (the binding site for a MarR regulator OhrR) (*20, 22*). They estimated the ST1−ST1710 binding constant to be ~15 μM using the gel mobility shift assay. Because of the low binding affinity, they suggested that the observed binding might be nonspecific. One factor that was not taken into consideration during the study described above is the temperature. ST1710 normally operates at 80 °C, and temperature is known to affect the interactions between DNA and protein (*36*−*38*). Binding constants determined at room temperature may not accurately reflect the real physiological values at 80 °C. In this study, we investigated the binding between ST1 and ST1710 at three temperatures, 10, 30, and 50 °C, using a different method (fluorescence polarization). The highest temperature for this study was limited by the instrumentation and the melting temperature of the double-stranded oligonucleotide containing the binding sequence. Since *S. tokodaii* thrives in the *Sulfolobus* medium, which has an ionic strength of ~0.04 M (calculated on the basis of the composition of the *Sulfolobus* medium), we included 50 mM NaCl in the binding buffer [10 mM HEPES (pH 7.5), 50 mM NaCl, and 1 μg/mL calf thymus DNA] (*39*). The forward sequence was labeled with FITC at the 5′-terminus and annealed with the reverse sequence to generate the FITC-labeled double-stranded DNA, F-ST1. Small aliquots of concentrated ST1710 were titrated into a solution containing 5 nM F-ST1, and the change in the fluorescence polarization (P) following the addition of the protein was monitored at all three temperatures (Figure 7). To evaluate the potential contribution of FITC to binding, ST1710 was titrated into a free FITC solution, and no increase in fluorescence polarization was observed (data not shown). The dissociation constant and the Hill coefficient were derived by fitting the binding data with the Hill equation as described in Materials and Methods (Table 1). Two conclusions could be made on the basis of the fitting results. First, the binding affinity increased with the increase in temperature. It was approximately doubled from 10 °C (K_d = 618 ± 34 nM) to 30 °C (K_d = 334 ± 15 nM) and from 30 to 50 °C (K_d = 189 ± 9 nM). Second, Hill coefficient n was close to 1 at all three temperatures, indicating the lack of cooperativity in binding. The melting of ST1 prevented us from conducting binding studies at even higher temperatures. If the binding affinity increased further with the increase in temperature, at 80 °C the dissociation constant might decrease to less than 100 nM. However, the lack of binding cooperativity is different from what has been observed for the bacterial MarR regulators, which clearly showed a positive cooperativity in DNA binding (*40*).

Small Ligands Repress the Binding between ST1710 and ST1. Using the ST1710−ST1 complexas a model system, we examined the inhibitory effect of CCCP and salicylate on protein−DNA binding at 50 °C (Figure 8A,B). Ethidium was excluded from this study due to its capability to intercalate into dsDNA. The fluorescence polarization of the ST1710−ST1 complex was monitored while small aliquots of concentrated ligands were titrated into the system. For both CCCP (Figure 8A) and salicylate (Figure 8B), the addition of ligands induced the dissociation of ST1710 and ST1, resulting in a decreased fluorescence polarization. No such effect was observed when the ligands were titrated into a solution of free ST1 (data not shown). To further investigate the specificity of this inhibitory effect, we checked the

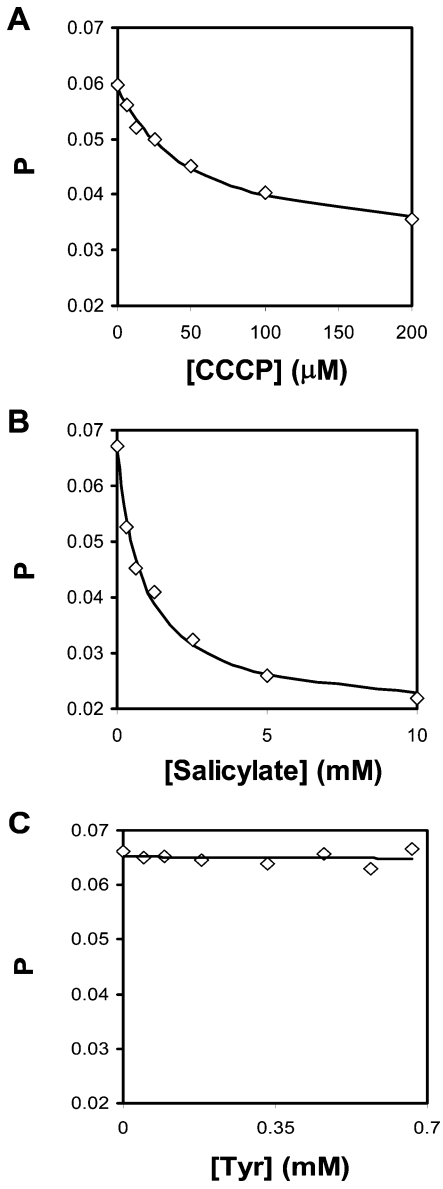

FIGURE 8: Effects of small molecule ligands CCCP (A), salycilate (B), and Tyr (C) on ST1710−DNA binding. The ligand was titrated into a buffer solution [10 mM HEPES, 50 mM NaCl (pH 7.5), and 1 μg/mL calf thymus DNA] containing 20 nM F-ST1 with 50 nM ST1710. Solid lines illustrate the trend of the data.

influence of the amino acid Tyr on ST1710−ST1 binding. Tyr contains a phenyl moiety, resembling the structure of salicylate. The concentration range we could test was limited by the poor solubility of Tyr in the binding buffer, but no repression was observed at the highest concentration used in this study (Figure 8C). Finally, we examined the binding between ST1710 and ST1 in the presence of a saturating concentration of salicylate. ST1710 was titrated into a solution of F-ST1 in the presence of 10 mM salicylate (K_d $\sim$ 1 mM), and no significant increase in fluorescence polarization signal was observed up to the highest protein concentration tested (5 μM) (data not shown). This result indicated that ST1710 did not interact with ST1 in the presence of the saturating concentration of salicylate.

In summary, we characterized the effector binding of an archaeal MarR-type repressor, ST1710, to three representative bacterial MarR ligands, including a cation, an anion, and a neutral molecule. Binding of these ligands caused conformational changes in the protein, as revealed by the near-UV CD spectra, the fluorescence emission of the reporter Trp residues, and the solvent accessibility of tyrosines in the protein structure. The binding affinities of the ligands for ST1710 were comparable to their affinities for the bacterial MarRs. For CCCP, one ligand bound to one ST1710 monomeric subunit. No cooperativity of binding was observed. Intriguingly, no cooperativity was observed for ST1710−ST1 binding either, which was different from what had been reported for the bacterial MarR-type repressor. Although it is possible that the archaeal MarR has a different mechanism, the high degree of structural similarity with the bacterial MarR argues against it. Since ST1 was identified using sequence homology rather than a more thorough study using DNA footprinting coupled with mutational experiments, there remains a possibility that ST1 does not contain the real promoter sequence of ST1710. The MarR regulators bind to (pseudo) palindromic sequences. No clear symmetry can be identified in the sequence of ST1. It is possible that part of the ST1 resembles half of the palindromic binding sequence, to which only one subunit of the ST1710 dimer binds efficiently. This may be the reason behind the lower-than-expected binding constant for a real promoter sequence and the lack of binding cooperativity. Nonetheless, the bindings of CCCP and salicylate clearly disrupt this interaction. The gene encoding ST1710 is downstream of gene *ST1709*, forming part of a bacterium-like operon. ST1709 is a putative multiple drug resistant transporter protein that belongs to the major facilitator superfamily. It is possible that both proteins are involved in functions such as detoxification or stress response, with ST1710 regulating the expression level of ST1709. The MarR family is one of the few regulator families that exists broadly in both the kingdoms of bacteria and archaea. As many archaea species are found in extremely hostile environments, it is not surprising that the MarR-type regulators would be critical for the survival of such organisms. An archaeal MarR activator, BldR, has been shown to play important roles in the detoxification of aromatic aldehyde (*41*). The exact cellular functions of ST1709 and ST1710 are still awaiting determination.

ACKNOWLEDGMENT

We acknowledge the use of the circular dichroism spectrometer and fluorescence spectrometer at the Protein Core Facility housed in the Department of Molecular and Cellular Biochemistry, University of Kentucky, and supervised by Dr. David Rodgers.

REFERENCES

1. Bell, S. D., Magill, C. P., and Jackson, S. P. (2001) Basal and regulated transcription in archaea. *Biochem. Soc. Trans. 29*, 392–395.
2. Hausner, W., Wettach, J., Hethke, C., and Thomm, M. (1996) Two transcription factors related with the eucaryal transcription factors TATA-binding protein and transcription factor IIB direct promoter recognition by an archaeal RNA polymerase. *J. Biol. Chem. 271*, 30144–30148.
3. Langer, D., Hain, J., Thuriaux, P., and Zillig, W. (1995) Transcription in archaea: Similarity to that in eucarya. *Proc. Natl. Acad. Sci. U.S.A. 92*, 5768–5772.
4. Soppa, J. (1999) Transcription initiation in archaea: Facts, factors and future aspects. *Mol. Microbiol. 31*, 1295–1305.

5. Best, A. A., and Olsen, G. J. (2001) Similar subunit architecture of archaeal and eukaryal RNA polymerases. *FEMS Microbiol. Lett. 195*, 85–90.
6. Bell, S. D., Kosa, P. L., Sigler, P. B., and Jackson, S. P. (1999) Orientation of the transcription preinitiation complex in archaea. *Proc. Natl. Acad. Sci. U.S.A. 96*, 13662–13667.
7. Kyrpides, N. C., and Ouzounis, C. A. (1999) Transcription in archaea. *Proc. Natl. Acad. Sci. U.S.A. 96*, 8545–8550.
8. Reeve, J. N. (2003) Archaeal chromatin and transcription. *Mol. Microbiol. 48*, 587–598.
9. Bell, S. D. (2005) Archaeal transcriptional regulation: Variation on a bacterial theme? *Trends Microbiol. 13*, 262–265.
10. Bell, S. D., and Jackson, S. P. (2001) Mechanism and regulation of transcription in archaea. *Curr. Opin. Microbiol. 4*, 208–213.
11. Geiduschek, E. P., and Ouhammouch, M. (2005) Archaeal transcription and its regulators. *Mol. Microbiol. 56*, 1397–1407.
12. George, A. M., and Levy, S. B. (1983) Amplifiable resistance to the tetracycline, chloramphenicol, and other antibiotics in *Escherichia coli*: Involvement of a nonplasmid-determined efflux of tetracycline. *J. Bacteriol. 155*, 531–540.
13. George, A. M., and Levy, S. B. (1983) Gene in the major cotransduction gap of the *Escherichia coli* K-12 linkage map required for the expression of chromosomal resistance to tetracycline and other antibiotics. *J. Bacteriol. 155*, 541–548.
14. Perez-Rueda, E., and Collado-Vides, J. (2001) Common history at the origin of the position-function correlation in transcriptional regulators in archaea and bacteria. *J. Mol. Evol. 53*, 172–179.
15. Perez-Rueda, E., Collado-Vides, J., and Segovia, L. (2004) Phylogenetic distribution of DNA-binding transcription factors in bacteria and archaea. *Comput. Biol. Chem. 28*, 341–350.
16. Wilkinson, S. P., and Grove, A. (2006) Ligand-responsive transcriptional regulation by members of the MarR family of winged helix proteins. *Curr. Issues Mol. Biol. 8*, 51–62.
17. Lim, D., Poole, K., and Strynadka, N. C. J. (2002) Crystal structure of the MexR repressor of the mexRAB-oprM multidrug efflux operon of *Pseudomonas aeruginosa*. *J. Biol. Chem. 277*, 29253–29259.
18. Wu, R. Y., Zhang, R. G., Zagnitko, O., Dementieva, I., Maltzev, N., Watson, J. D., Laskowski, R., Gornicki, P., and Joachimiak, A. (2003) Crystal structure of *Enterococcus faecalis* SlyA-like transcriptional factor. *J. Biol. Chem. 278*, 20240–20244.
19. Saridakis, V., Shahinas, D., Xu, X. H., and Christendat, D. (2008) Structural insight on the mechanism of regulation of the MarR family of proteins: High-resolution crystal structure of a transcriptional repressor from *Methanobacterium thermoautotrophicum*. *J. Mol. Biol. 377*, 655–667.
20. Hong, M., Fuangthong, M., Helmann, J. D., and Brennan, R. G. (2005) Structure of an OhrR-*ohrA* operator complex reveals the DNA binding mechanism of the MarR family. *Mol. Cell 20*, 131–141.
21. Alekshun, M. N., Levy, S. B., Mealy, T. R., Seaton, B. A., and Head, J. F. (2001) The crystal structure of MarR, a regulator of multiple antibiotic resistance, at 2.3 angstrom resolution. *Nat. Struct. Biol. 8*, 710–714.
22. Kumarevel, T., Tanaka, T., Nishio, M., Gopinath, S. C. B., Takio, K., Shinkai, A., Kumar, P. K. R., and Yokoyama, S. (2008) Crystal structure of the MarR family regulatory protein, ST 1710, from *Sulfolobus tokodaii* strain. *J. Struct. Biol. 161*, 9–17.
23. Miyazono, K. I., Tsujimura, M., Kawarabayasi, Y., and Tanokura, M. (2007) Crystal structure of an archaeal homologue of multidrug resistance repressor protein, EmrR, from hyperthermophilic archaea *Sulfolobus tokodaii* strain 7. *Proteins: Struct., Funct., Bioinf. 67*, 1138–1146.
24. Lundblad, J. R., Laurance, M., and Goodman, R. H. (1996) Fluorescence polarization analysis of protein-DNA and protein-protein interactions. *Mol. Endocrinol. 10*, 607–612.
25. Hugli, T. E., and Stein, W. H. (1971) Involvement of a tyrosine residue in activity of bovine pancreatic deoxyribonuclease A. *J. Biol. Chem. 246*, 7191–7200.
26. Riordan, J. F., Sokolovs, M., and Vallee, B. L. (1967) Functional tyrosyl residues of carboxypepridase A. Nitration with tetranitromethane. *Biochemistry 6*, 3609–3617.
27. Riordan, J. F., Sokolovs, M., and Vallee, B. L. (1967) Environmentally sensitive tyrosyl residues. Nitration with tetranitromethane. *Biochemistry 6*, 358–361.
28. Kahn, P. C. (1979) The interpretation of near-ultraviolet circular dichroism. *Methods Enzymol. 61*, 339–378.
29. Strickland, E. H., and Mercola, D. (1976) Near-ultraviolet tyrosyl circular-dichroism of pig insulin monomers, dimmrs, and hexamers: Dipole-dipole coupling calculations in monopole approximation. *Biochemistry 15*, 3875–3884.
30. Kelly, S. M., and Price, N. C. (2000) The application of circular dichroism to studies of protein folding and unfolding. *Biochim. Biophys. Acta 1338*, 161–185.
31. Noble, M. A., Munro, A. W., Rivers, S. L., Robledo, L., Daff, S. N., Yellowlees, L. J., Shimizu, T., Sagami, I., Guillemette, J. G., and Chapman, S. K. (1999) Potentiometric analysis of the flavin cofactors of neuronal nitric oxide synthase. *Biochemistry 38*, 16413–16418.
32. Andersson, L. A., and Peterson, J. A. (1995) Active-site analysis of ferric P450 enzymes: Hydrogen-bonding effects on the circular dichroism spectra. *Biochem. Biophys. Res. Commun. 211*, 389–395.
33. Cogdell, R. J., Isaacs, N. W., Freer, A. A., Arrelano, J., Howard, T. D., Papiz, M. Z., Hawthornthwaite-Lawless, A. M., and Prince, S. (1997) The structure and function of the LH2 (B800−850) complex from the purple photosynthetic bacterium *Rhodopseudomonas acidophila* strain 10050. *Prog. Biophys. Mol. Biol. 68*, 1–27.
34. Cogdell, R. J., and Scheer, H. (1985) Circular-dichroism of light-harvesting complexes from purple photosynthetic bacteria. *Photochem. Photobiol. 42*, 669–678.
35. West, S. M., and Price, N. C. (1990) The unfolding and attemped refolding of mitochondrial aspartate-aminotransferase from pig-heart. *Biochem. J. 265*, 45–50.
36. Berezovski, M., and Krylov, S. N. (2005) Thermochemistry of protein-DNA interaction studied with temperature-controlled non-equilibrium capillary electrophoresis of equilibrium mixtures. *Anal. Chem. 77*, 1526–1529.
37. Liu, C. C., Richard, A. J., Datta, K., and LiCata, V. J. (2008) Prevalence of temperature-dependent heat capacity changes in protein-DNA interactions. *Biophys. J. 94*, 3258–3265.
38. Peters, W. B., Edmondson, S. P., and Shriver, J. W. (2004) Thermodynamics of DNA binding and distortion by the hyperthermophile chromatin protein Sac7d. *J. Mol. Biol. 343*, 339–360.
39. Suzuki, T., Iwasaki, T., Uzawa, T., Hara, K., Nemoto, N., Kon, T., Ueki, T., Yamagishi, A., and Oshima, T. (2002) *Sulfolobus tokodaii* sp nov (f. *Sulfolobus* sp strain 7), a new member of the genus *Sulfolobus* isolated from Beppu Hot Springs, Japan. *Extremophiles 6*, 39–44.
40. Oh, S. Y., Shin, J. H., and Roe, J. H. (2007) Dual role of OhrR as a repressor and an activator in response to organic hydroperoxides in *Streptomyces coelicolor*. *J. Bacteriol. 189*, 6284–6292.
41. Fiorentino, G., Ronca, R., Cannio, R., Rossi, M., and Bartolucci, S. (2007) MarR-like transcriptional regulator involved in detoxification of aromatic compounds in *Sulfolobus solfataricus*. *J. Bacteriol. 189*, 7351–7360.
42. Alekshun, M. N., and Levy, S. B. (1999) Alteration of the repressor activity of MarR, the negative regulator of the *Escherichia coli* marRAB locus, by multiple chemicals in vitro. *J. Bacteriol. 181*, 4669–4672.
43. Xiong, A., Gottman, A., Park, C., Baetens, M., Pandza, S., and Matin, A. (2000) The EmrR protein represses the *Escherichia coli* emrRAB multidrug resistance operon by directly binding to its promoter region. *Antimicrob. Agents Chemother. 44*, 2905–2907.
44. Brooun, A., Tomashek, J. J., and Lewis, K. (1999) Purification and ligand binding of EmrR, a regulator of a multidrug transporter. *J. Bacteriol. 181*, 5131–5133.
45. Poirot, O., O'Toole, E., and Notredame, C. (2003) Tcoffee@igs: A web server for computing, evaluating and combining multiple sequence alignments. *Nucleic Acids Res. 31*, 3503–3506.

BI801662S